Liquid Crystals
Publication details, including instructions for authors and subscription information:
http://www.informaworld.com/smpp/title~content=t713926090

Photochemical tuning capability of cholesteric liquid crystal cells containing chiral dopants end capped with menthyl groups

Jui-Hsiang Liu[a]; Po-Chih Yang[a]; Hsien-Jung Hung[a]; Der-Jang Liaw
[a] Department of Chemical Engineering, National Cheng Kung University, Tainan 70101, Taiwan, ROC

To cite this Article Liu, Jui-Hsiang , Yang, Po-Chih , Hung, Hsien-Jung and Liaw, Der-Jang(2007) 'Photochemical tuning capability of cholesteric liquid crystal cells containing chiral dopants end capped with menthyl groups', Liquid Crystals, 34: 7, 891 — 902
To link to this Article: DOI: 10.1080/02678290701407185
URL: http://dx.doi.org/10.1080/02678290701407185

Liquid Crystals, Vol. 34, No. 7, July 2007, 891–902

Photochemical tuning capability of cholesteric liquid crystal cells containing chiral dopants end capped with menthyl groups

JUI-HSIANG LIU*†, PO-CHIH YANG†, HSIEN-JUNG HUNG† and DER-JANG LIAW‡

†Department of Chemical Engineering, National Cheng Kung University, Tainan 70101, Taiwan, ROC
‡Department of Chemical Engineering, National Taiwan University of Science and Technology, Taiwan, ROC

(*Received 11 September 2006; accepted 1 January 2007*)

In order to investigate the photochemical tuning capability of chiral monomers and polymers containing end-capped menthyl groups, a new series of chiral dopants was synthesized and added to commercially available nematic liquid crystals to induce cholesteric liquid crystal (LC) phases. The addition of chiral dopants with azo structure led to phototunability of the reflection colour of the LC cells. Photochromic variation of the LC cells due to photoisomerization of the azo compound was investigated. After photopolymerization of the monomers inside the cholesteric LC cells, the centre wavelength of the reflected band of the incident light was found to be fixed and the reflected bandwidth was broadened, resulting in a red shift. A schematic representation of both the photoisomerization of the azo dopants and its effect on variation of twisting pitches is proposed. Real image recording was performed using 365 nm UV through a mask with text. The top and side views of the morphological network structures of a fabricated cholesteric LC cell were investigated using scanning electron microscopy. The results of this investigation demonstrated that RGB reflected colours of LC cells can easily be achieved through the addition of the menthyl-containing synthesized chiral compounds to nematic LCs. The addition of synthesized AzoM helped further in recording the patterns onto cholesteric LC films using 365 nm UV exposure.

1. Introduction

In recent years, a new approach for the development of chiral nematic (or cholesteric) low molar mass [1–4] and polymeric materials showing light-induced and controllable changes in helical pitch lengths has been reported [5, 6]. This approach is based on the introduction of chiral photosensitive fragments into the nematic matrix. These fragments undergo light-induced *E–Z* photoisomerization. As a result of this process, Z-isomerization of the chiral photochromic groups takes place. This isomerization is accompanied by a decrease in the anisometry of the photochromic groups and, as a consequence, results in a decrease in their helical twisting power. Therefore, upon light irradiation, the macroscopic chirality of the system is reduced and, in the case of systems containing a single chiral component, the helical pitch length increases. Such systems appear to be attractive from the viewpoint of their practical application potential, because, upon light irradiation and the concurrent untwisting of the cholesteric helix, the selective light reflection maximum is shifted to a longer wavelength region of the spectrum. Hence, the optical properties of films based on such systems may be easily controlled by light irradiation via local variations in the selective light reflection wavelength.

Many publications have been devoted to studies of the preparation and applications of photosensitive liquid crystal (LC) polymers containing a chiral terminal moiety (see, for example, Bobrovsky *et al.* [7] and van de Witte *et al.* [8]). The working principle of photocontrollable cholesteric polymers was the introduction of photosensitive or photoisomerized mesogenic fragments, such as azobenzene and stilbene, which could reverse their configuration when irradiated with light of different wavelengths. When the configuration changed, the twisting power or optical characteristics also changed. Composite films were photoirradiated at different wavelengths to bring about the photoisomerization of the guest azobenzene. Azobenzene is an attractive photosensitive material because of its simple photochemistry and ease of chemical modification. Azobenzene dissolved in a chiral nematic (cholesteric) LC provided photocontrollability of the helical pitches as a result of *E–Z* photoisomerization, as demonstrated by Sackmann [9]. On the other hand, a chiral azobenzene derivative dissolved in a nematic LC can

*Corresponding author. Email: jhliu@mail.ncku.edu.tw

Liquid Crystals
ISSN 0267-8292 print/ISSN 1366-5855 online © 2007 Taylor & Francis
http://www.tandf.co.uk/journals
DOI: 10.1080/02678290701407185

act both as a chiral dopant to induce a chiral nematic phase and a phototrigger to control the generated helical pitch [10, 11].

A cholesteric structure is characterized by its handedness and pitch. Equal amounts of enantiomeric 'guests' of equal enantiomeric purity induce helical structures with identical pitch and opposite handedness [12]. Different substances show a different ability to twist a nematic phase. The ability of a chiral dopant to induce helical pitch is quantitatively defined as helical twisting power, β. The helical twisting power of chiral compounds can be defined as the slope of the plot of $1/p$ (p=pitch) versus the concentration of the chiral compound [13–15]. In theory, many factors can influence the pitch of cholesteric LCs, e.g. the molecular chirality, the chemical structure of the chiral moiety, the molecular interaction between host and guest molecules, etc.

In a series of investigations on cholesteric LCs, the synthesis of chiral dopants and chiral polymers has been discussed. Their optical properties and applications to LC cells and recording films were also studied [16–20]. Chiral monomers and polymers with end-capped menthyl groups were newly synthesized in the earlier study [21]. In order to study the photochemical tuning capability of chiral monomers and polymers, the synthesized menthyl-containing chiral dopants were added to commercially available nematic LCs to induce cholesteric LC phases. In this investigation, it was found that after UV polymerization, the pitch of the cholesteric LC cells was fixed and the reflective bandwidth broadened. RGB reflection colours of the LC cells could be obtained easily using the chiral dopants synthesized in this investigation. The dependence of the twisting pitches of the cholesteric LC cells on the molecular structure and concentration was also investigated. Real image recording of the cholesteric LC cells was achieved using UV exposure through a mask with text.

2. Experimental

2.1. *Measurements*

FTIR spectra were recorded on a Jasco VALOR III (Tokyo, Japan) FTIR spectrophotometer. Nuclear magnetic resonance (NMR) spectra were obtained on a Bruker AMX-400 (Darmstadt, Germany) high-resolution NMR spectrometer. The optical rotation of chiral compounds was measured with a Jasco DIP-370 using the D-line of sodium (λ=589 nm). Measurements were performed using 1% solutions of substances in chloroform. Elemental analyses were conducted with a Heraeus CHN-O (Darmstadt, Germany) rapid elemental analyser. Differential scanning calorimetry (DSC) was conducted with a Perkin-Elmer DSC 7 instrument at heating and cooling rates of 10 K min^{-1} in a nitrogen atmosphere. The phase transitions were investigated with an Olympus BH-2 polarizing optical microscope (POM) equipped with Mettler hot stage FP-82; the temperature scanning rate was set at 10 K min^{-1}. UV spectroscopy measurements were carried out with a Jasco V-550 UV-Vis spectrophotometer. The transmittance spectra were recorded with a USB-2000 fibre optic spectrometer from Oceanoptics Company. UV light (365 nm) with an intensity of 0.4 mW was used as a pumping light to induce isomerization of azo molecules in the cholesteric LC systems. Scanning electron microscope (SEM) microphotographs were obtained with a Jeol HR-FESEM JSM-6700F (Osaka, Japan) instrument.

2.2. *Materials*

ZLI-2293, a commercially available eutectic mixture of several low molar mass nematic LCs, was purchased from Merck (Darmstadt, Germany) and was used as an LC host without further purification. This LC exhibits a nematic phase over a wide range of temperature up to 85°C. The chiral monomers and azobenzene derivative used in this investigation are shown in scheme 1 and were synthesized during previous work; they were all identified using spectrophotometers. Chiral agent S811 was purchased from Merck; it induces a left-handed helical structure, and was also dissolved in the host nematic LC to produce a cholesteric LC phase. The bifunctional monomer BAHB, 4,4′-bis[6-(acryloyloxy)-hexyloxy]biphenyl, was synthesized by a reported method [22]. Photoinitiator BME (benzoin methyl ether) was purchased from Acros (Geel, Belgium).

2.3. *Fabrication of liquid crystal cells*

ITO-coated plates were cleaned with detergent solution, washed with water and then with acetone using ultrasonic equipment for 20 min and 60 min, respectively. After completion of the cleaning process, the ITO plates were dried in vacuum. The surface of the ITO plates was coated with polyvinyl alcohol (M_w=20 000), dried and then rubbed. A glass cell with a pair of parallel pre-rubbed ITO plates and a gap of 12 µm was fabricated. After filling with LC mixture, the ITO cell was sealed with epoxy resin.

The LC composite cells were prepared from a mixture of ZLI-2293/chiral dopant/azobenzene derivative or ZLI-2293/S811/mono-/bifunctional monomer/BME (photoinitiator). The bifunctional monomer BAHB was used as a crosslinking agent. Since ZLI-2293 is a

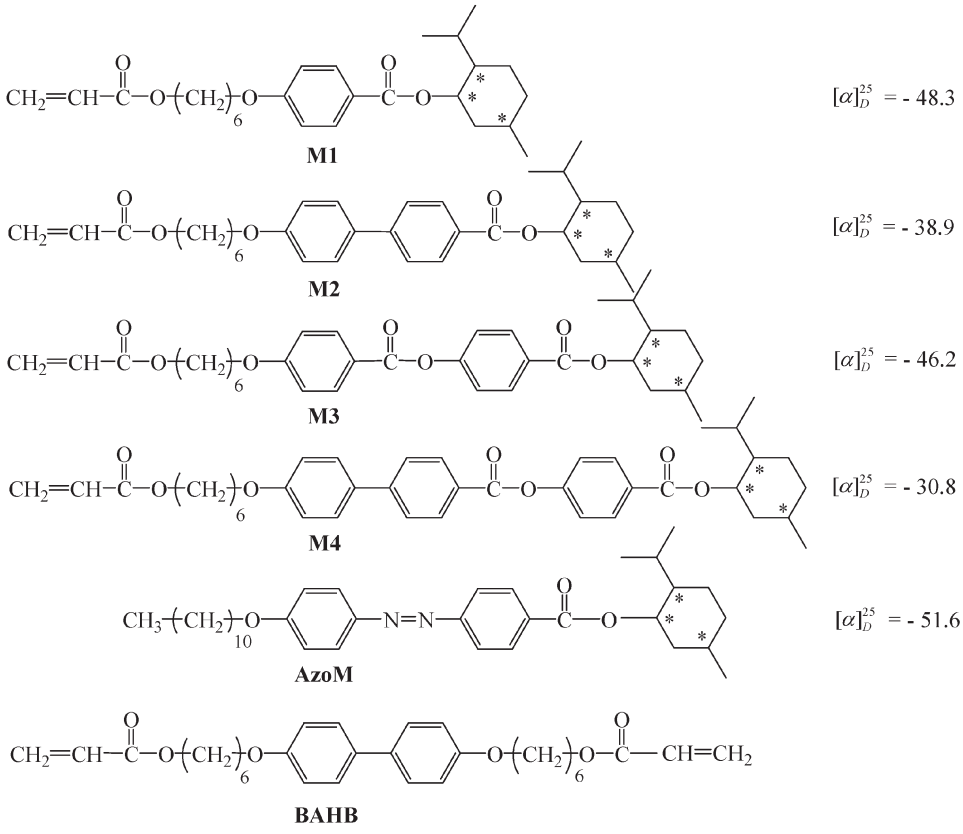

Scheme 1. Chiral monomers and azobenzene derivative used.

nematic LC mixture, the composition of which is complex, for convenience, weight ratios of ZLI-2293/S811/mono- and bifunctional monomer were used. To prepare LC composite cells, sample cells with the monomer/LC mixture were cured by UV irradiation at 0.65 mW cm^{-2}. After completion of the polymerization, LC composite films were fabricated, assisted by the surface treatment of the substrates, and the pitch length of the cholesteric LC determined. The optical properties of the LC cells were also investigated. Morphological observation of the solid polymer in the composite films was performed by SEM.

2.4. *Syntheses of monomers*

The chemical structures of the chiral monomers and azobenzene derivative are shown in scheme 1. The following novel chiral monomers were synthesized according to similar procedures described in the literature [16, 23–26]. The synthesized products were purified and then identified using FTIR and ^{1}H NMR.

2.4.1. 4-(6-Hydroxyhexyloxy)benzoic acid (1). Yield: 19.1 g (67%), T_m=139–140°C. FTIR (cm^{-1}): 3249 (OH), 2932, 2856 (CH_2), 1685 (C=O in Ar–COO–), 1600, 1521 (C–C in Ar), 1287, 1251 (COC), 2681, 2561 (COOH). ^{1}H NMR (DMSO-d_6, δ in ppm): 1.28–1.74 (m, 8H, CH_2), 3.32 (m, 2H, OCH_2CH_2), 4.01 (m, 2H, CH_2OPh), 6.99–7.87 (m, 4H, aromatic), 12.6 (1H, –COOH).

2.4.2. 4-(6-Acryloyloxyhexyloxy)benzoic acid (2). Yield: 6.3 g (69%), Cr 88°C N 92°C I. FTIR (cm^{-1}): 2933, 2854 (CH_2), 1733 (C=O in Ar–COO–), 1604, 1528 (C–C in Ar), 1291, 1246 (COC), 2672, 2566 (COOH), 1685 (C=C). ^{1}H NMR(DMSO-d_6, δ in ppm): 0.94–1.28 (m, 8H, CH_2), 4.05 (m, 2H, CH_2OPh), 4.12 (m, 2H, $COOCH_2$), 5.44 (dd, 1H, CH_2=CH), 5.68 (dd, 1H, CH_2=CH), 5.86 (dd, 1H, CH_2=CH), 6.53–7.40 (m, 4H, aromatic), 12.5 (1H, –COOH).

2.4.3. 4-Menthyl 4-(6-acryloyloxyhexyloxy)benzoate (M1) (3). Yield: 2.45 g (57%). T_m=10.4°C. FTIR (cm^{-1}): 2930, 2869 (CH_2), 1732 (C=O in Ar–COO–), 1604, 1510 (C–C in Ar), 1257, 1198 (COC), 1638 (C=C). ^{1}H NMR ($CDCl_3$, δ in ppm): 0.86–0.96 (m, 9H, CH_3), 1.26–1.42 (m, 17H, CH_2), 4.0 (d, 2H, CH_2OPh), 4.17 (d, 2H, $COOCH_2$), 4.90 (m, 1H, $OCHCH_2$), 5.81 (dd, 1H, CH_2=CH), 6.12 (dd, 1H, CH_2=CH), 6.38 (dd,

1H, CH_2=CH), 6.90 (d, 2H, aromatic), 7.98 (d, 2H, aromatic).

2.4.4. 4-(6-Hydroxyhexyloxy) biphenyl-4′-carboxylic acid (4). Yield: 12.5 g (57%). T_m=200–201°C. FTIR (cm^{-1}): 3227 (OH), 2932, 2851 (CH_2), 1684 (C=O in Ar–COO–), 1600, 1506 (C–C in Ar), 1289, 1251 (COC), 2686, 2556 (COOH). ^{1}H NMR (d-acetone, δ in ppm): 1.42–1.84 (m, 8H, CH_2), 3.54 (m, 2H, OCH_2CH_2), 4.06 (m, 2H, CH_2OPh), 7.03 (d, 2H, aromatic), 7.58 (d, 2H, aromatic), 7.70 (d, 2H, aromatic), 8.06 (d, 2H, aromatic).

2.4.5. 4-(Acryloyloxyhexyloxy)biphenyl-4′-carboxylic acid (5). Yield: 10.1 g (72%). T_m=140–141°C. FTIR (cm^{-1}): 2933, 2854 (CH_2), 1733 (CO in Ar–COO–), 1604, 1528 (C–C in Ar), 1291, 1246 (COC), 2672, 2566 (COOH), 1685 (C=C). ^{1}H NMR (DMSO, δ in ppm): 1.34–1.76 (m, 8H), 4.01 (m, 2H, CH_2OPh), 4.18 (m, 2H, $COOCH_2$), 5.90 (dd, 1H, CH_2=CH), 6.16 (dd, 1H, CH_2=CH), 6.32 (dd, 1H, CH_2=CH), 7.03 (d, 2H, aromatic), 7.65 (d, 2H, aromatic), 7.74 (d, 2H, aromatic), 7.97 (d, 2H, aromatic).

2.4.6. Menthyl 4-(acryloyloxyhexyloxy)biphenyl-4′-carboxylate (M2) (6). Yield: 2.38 g (47%). T_m=60.5°C. FTIR (cm^{-1}): 2931, 2856 (CH_2), 1730 (CO in Ar–COO–), 1608, 1524 (C–C in Ar), 1285, 1240 (COC), 1697 (C=C). ^{1}H NMR ($CDCl_3$, δ in ppm): 0.79–0.94 (m, 9H, CH_3), 0.92–2.16 (m, 17H), 4.01 (m, 2H, CH_2OPh), 4.18 (m, 2H, $COOCH_2$), 4.94 (m, 1H, $OCHCH_2$), 5.81 (dd, 1H, CH_2=CH), 6.12 (dd, 1H, CH_2=CH), 6.40 (dd, 1H, CH_2=CH), 6.97 (d, 2H, aromatic), 7.55 (d, 2H, aromatic), 7.61 (d, 2H, aromatic), 8.07 (d, 2H, aromatic).

2.4.7. 4-(Methoxycarbonyloxy)benzoic acid [26] (7). Yield: 16.1 g (82.1%). T_m=175°C. FTIR (cm^{-1}): 2961,

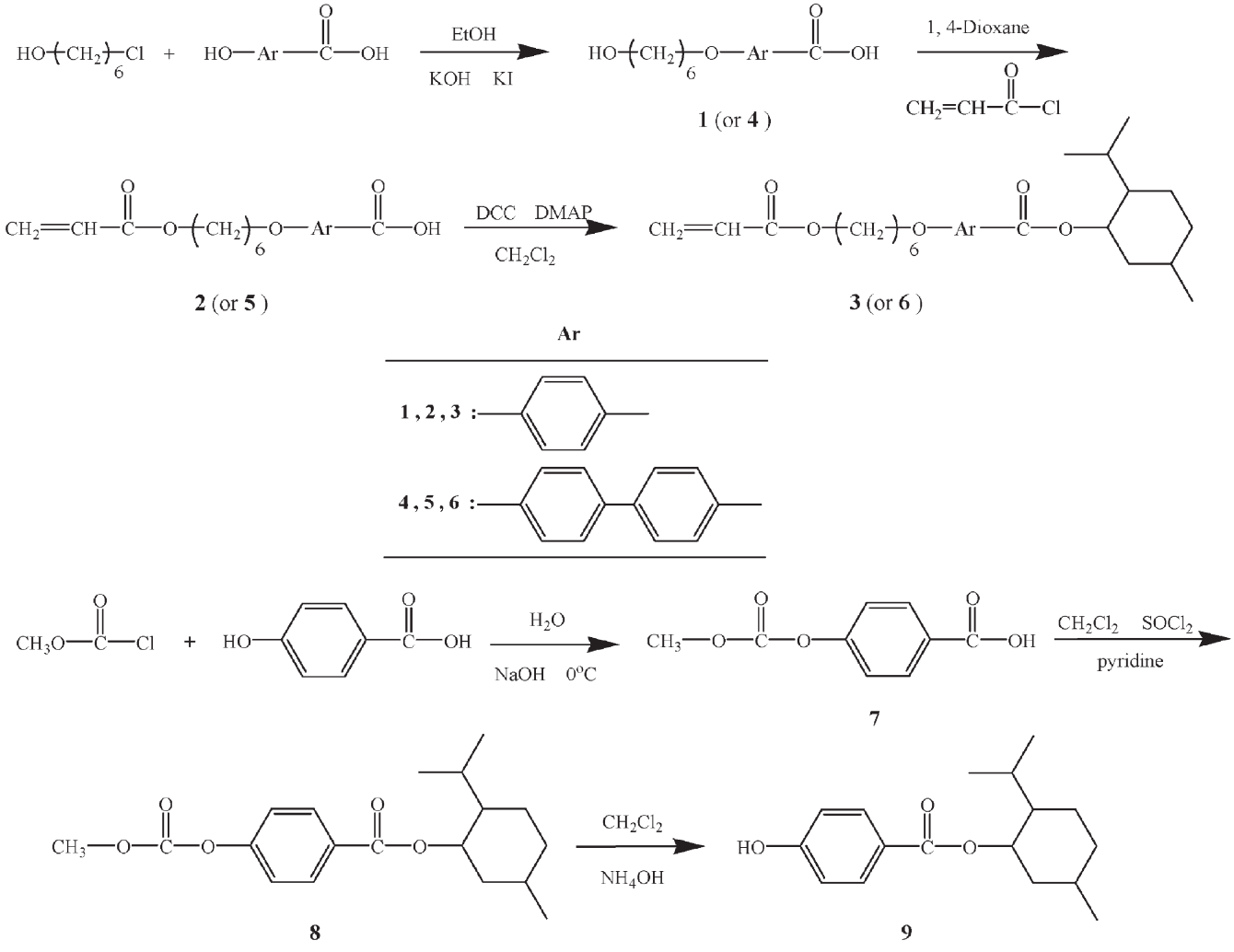

Scheme 2. Synthesis of chiral monomers.

2895 (CH_2), 1693 (C=O in Ar–COO–), 1608, 1503 (C–C in Ar), 2680, 2555 (COOH). ^{1}H NMR (d-acetone, δ in ppm): 3.85 (m, 3H, CH_3O), 7.34 (d, 2H, aromatic), 8.12 (d, 2H, aromatic), 10.16 (COOH).

2.4.8. Menthyl 4-(methoxycarbonyloxy)benzoate (8). Yield: 5.43 g (45.2%). FTIR (cm^{-1}): 2950, 2875 (CH_2), 1705 (C=O in Ar–COO–), 1608, 1503 (C–C in Ar). ^{1}H NMR ($CDCl_3$, δ in ppm): 0.84–0.96 (m, 9H, CH_3), 0.98–1.86 (m, 9H, CH_2), 3.79 (m, 3H, CH_3O), 4.94 (m, 1H, $OCHCH_2$), 7.24 (d, 2H, aromatic), 8.26 (d, 2H, aromatic).

2.4.9. Menthyl 4-hydroxybenzoate (9). Yield: 2.64 g (67.2%), T_m=92.5°C. FTIR (cm^{-1}): 3347 (OH), 2947, 2872 (CH_2), 1686 (C=O in Ar–COO–), 1602, 1511 (C–C in Ar), 1220, 1281 (COC). ^{1}H NMR (d-acetone, δ in ppm): 0.78–0.90 (m, 9H, CH_3), 0.92–1.88 (m, 9H, CH_2), 4.82–4.90 (m, 1H, $OCHCH_2$), 6.88–6.91 (d, 2H, aromatic), 7.86–7.90 (d, 2H, aromatic).

2.4.10. Menthyl 4-(6-acryloyloxyhexyloxy)phenyl-4-6-acryloyloxyhexyloxy)phenyl-4′-benzoate (M3) (10). Yield: 1.85 g (42.0%). T_m=32.6°C. FTIR (cm^{-1}): 2934, 2870 (CH_2), 1712 (C=O in Ar–COO–), 1610, 1505 (C–C in Ar), 1196, 1230 (COC), 1630 (C=C). ^{1}H NMR ($CDCl_3$, δ in ppm): 0.77–0.82 (m, 9H, CH_3), 0.89–1.91 (m, 17H, CH_2), 4.04 (d, 2H, CH_2OPh), 4.18 (d, 2H, $COOCH_2$), 4.90–4.97 (m, 1H, $OCHCH_2$), 6.96–6.99 (d, 2H, aromatic), 7.26–7.29 (d, 2H, aromatic), 8.01–8.16 (m, 4H, aromatic).

2.4.11. Menthyl 4-(6-acryloyloxyhexyloxy)biphenyl-4′-carbonyloxybenzoate (M4) (11). Yield: 2.20 g (70.4%). T_m=98.3°C. FTIR (cm^{-1}): 2942, 2865 (CH_2), 1720 (C=O in Ar–COO–), 1615, 1508 (C–C in Ar), 1265, 1230 (COC), 1632 (C=C). ^{1}H NMR ($CDCl_3$, δ in ppm): 0.77–0.89 (m, 9H, CH_3), 0.92–2.06 (m, 17H, CH_2), 4.03 (d, 2H, CH_2OPh), 4.18 (d, 2H, $COOCH_2$), 4.90–4.99 (m, 1H, $OCHCH_2$), 6.99–7.02 (d, 2H, aromatic), 7.29–7.32 (d, 2H, aromatic), 7.58–7.71 (m, 4H, aromatic), 8.12–8.25 (m, 4H, aromatic).

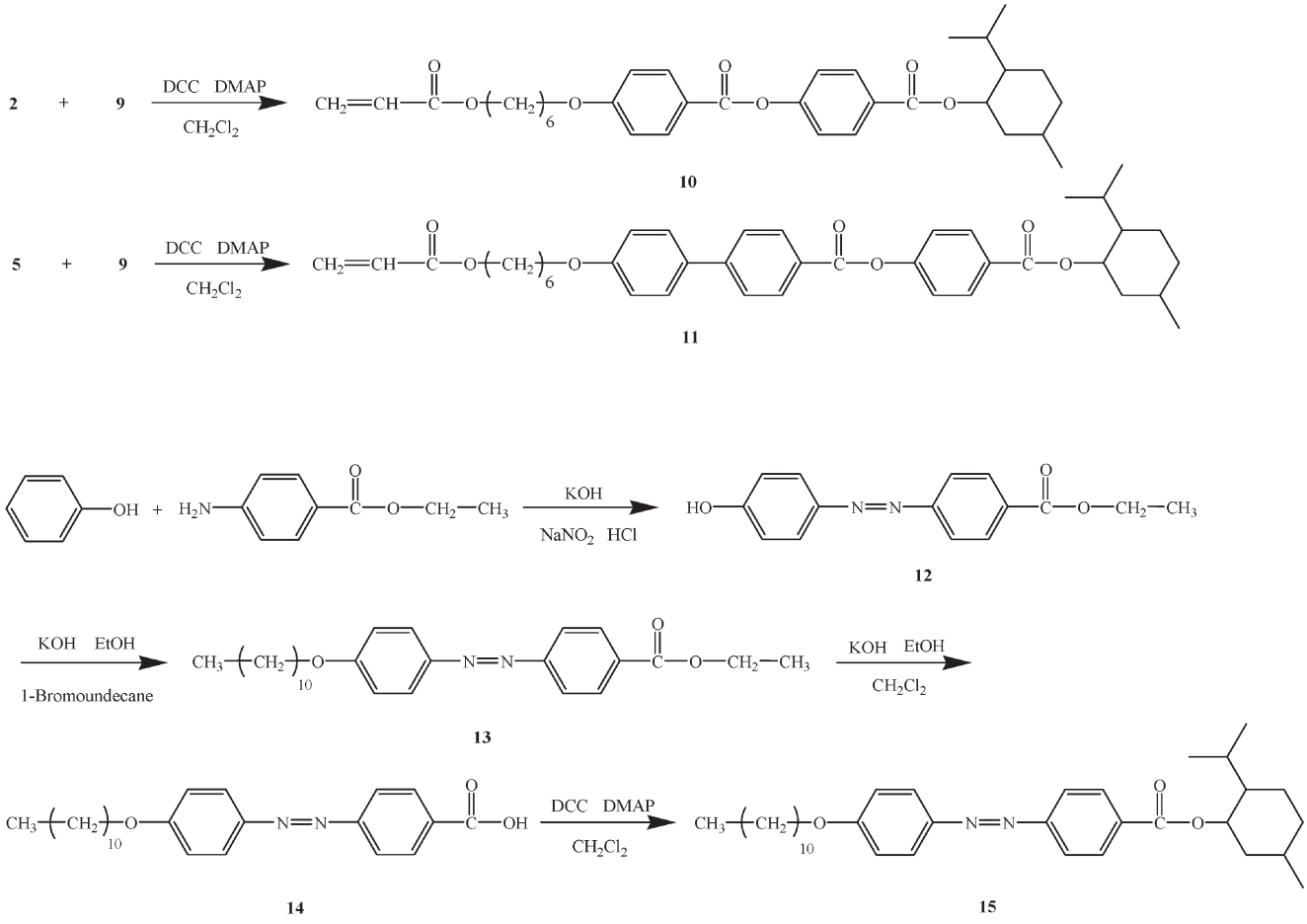

Scheme 3. Synthesis of photochromic azo compound.

Table 1. Phase transition temperature (°C), enthalpy changes ($J\,g^{-1}$)[a] and specific rotation of compounds (Cr=crystal, I=isotropic).

Sample	Heating cycle	Cooling cycle	$[\alpha]_D^{25}$[b]
M1	Cr 10.4 (15.6) I	I 0.5 (−6.4) Cr	−48.3
M2	Cr 60.5 (108.2) I	I 31.5 (−56.2) Cr	−38.9
M3	Cr 32.6 (25.4) I	I 12.5 (−7.9) Cr	−46.2
M4	Cr 98.3 (65.6) I	I 43.8 (−2.8) Cr	−30.8
Azo M	Cr 71.7 (64.8) I	I 42.8 (−62.4) Cr	−51.6

[a]Enthalpy of the phase change during heating and cooling at a rate of 10 K min^{-1}. [b]Specific rotation of compounds, 0.1 g in 10 ml $CHCl_3$.

2.4.12. 4-Hydroxy-4′-ethoxycarbonylazobenzol (12). Yield: 11.8 g (72%). T_m=153–154°C. FTIR (cm^{-1}): 3399 (OH), 2973, 2927, 2906 (CH_2), 1693 (C=O in Ar–COO–), 1601, 1504 (C–C in Ar). ^{1}H NMR ($CDCl_3$, δ in ppm): 1.38 (t, 3H, OCH_2CH_3), 4.35 (d, 2H, OCH_2), 7.03–8.17 (m, 8H, aromatic).

2.4.13. Ethyl 4-(4-undecyloxyphenylazo)benzoate (13). Yield: 9.42 g (74%). Cr 90.0°C SmA 96.3°C I (cooling). FTIR (cm^{-1}): 2950, 2855 (CH_2), 1690 (C=O in Ar–COO–). ^{1}H NMR (acetone-*d*6, δ in ppm): 0.85–0.90 (m, 3H, CH_3), 1.08–1.24 (m, 18H, –CH_2), 1.37–1.40 (t, 3H, OCH_2CH_3), 4.02 (d, 2H, OCH_2Ph), 4.15 (d, 2H, OCH_2), 7.05–7.08 (d, 2H, aromatic), 7.78–7.92 (m, 4H, aromatic), 8.12–8.16 (d, 2H, aromatic).

2.4.14. 4-(4-Undecyloxyphenylazo)benzoic acid (14). Yield: 8.03 g (81.0%). FTIR (cm^{-1}): 2945, 2852 (CH_2), 1689 (C=O in Ar–COO–). ^{1}H NMR (acetone-*d*6, δ in ppm): 0.87–1.97 (m, 21H, –$C_{10}H_{21}$), 4.04 (d, 2H, OCH_2Ph), 7.10–7.12 (d, 2H, aromatic), 7.86–7.94 (m, 4H, aromatic), 8.12–8.14 (d, 2H, aromatic).

2.4.15. Menthyl 4-(4-undecyloxyphenylazo)benzoate (AzoM) (15). Yield: 1.76 g (33.0%). T_m=71.7°C. FTIR (cm^{-1}): 2954, 2860 (CH_2), 1702 (C=O in Ar–COO–). ^{1}H NMR ($CDCl_3$, δ in ppm): 0.75–0.82 (m, 9H, CH_3), 0.96–1.48 (m, 27H, CH_2), 4.03 (d, 2H, CH_2OPh), 4.95 (m, 1H, $OCHCH_2$), 7.00–7.02 (d, 2H, aromatic), 7.89–7.98 (m, 4H, aromatic), 8.15–8.17 (d, 2H, aromatic).

3. Results and discussion

In order to investigate the photochemical tuning capability of the chiral monomers and polymers, a series of chiral dopants was synthesized and added to commercially available nematic LC to induce cholesteric LC phases. Schemes 1–3 show the molecular structures and the synthetic procedures for the synthesized monomers and photochromic azo compound. All the synthesized compounds were identified using ^{1}H NMR, FTIR and elemental analysis. To increase the polymerization rate, bifunctional monomer BAHB was synthesized and added to the LC composition for fabrication and investigation of cholesteric LC cells.

The phase transition temperatures and specific rotation of the chiral monomers and azobenzene derivatives were estimated using a differential scanning calorimeter and a polarimeter, respectively. The results are summarized in table 1. None of the chiral monomers or the azo compound with a chiral end-capped menthyl group exhibited liquid crystalline phases. In general, the existence of a highly sterically hindered molecular structure might disturb molecular orientation, leading to the absence of the liquid crystalline phases. The temperature variation between the heating and cooling cycles might be due to delay in molecular reorientation. As shown in scheme 1, the difference in both steric hindrance and polarity between the chiral compounds is quite large. Intermolecular forces and molecular polarity usually determine the thermal properties and the specific rotation, respectively. A menthyl group was introduced into the compounds through an –OH bond. This did not break the chiral centres in the menthyl groups; thus for every chiral

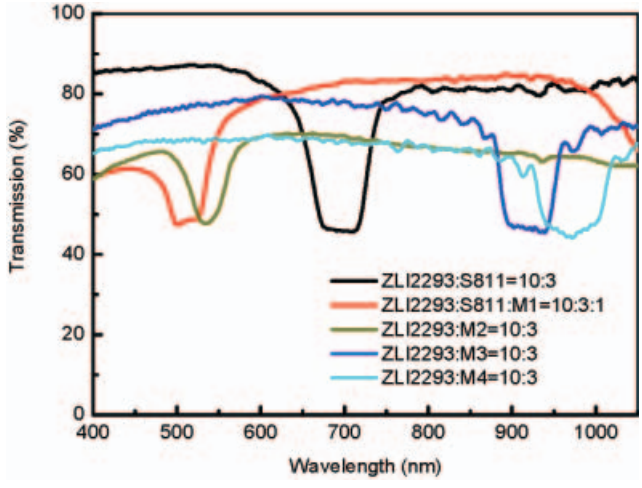

Figure 1. Effect of various chiral dopants on the cholesteric LC cells.

Table 2. Effect of chiral dopants on reflection wavelength of cholesteric cells.

		Before UV				
Entry	Chiral dopant [a]	λ_o [b]	$\Delta\lambda$ [c]	p [d]	HTP [e]	$T_{Ch\text{-}I}$/°C [f]
1	S811 [h]	695	105	444	9.9	72
2	M1	– [g]	–	–	–	–
3	S811/M1(3:1)	512	96	327	10.7	50
4	M2	530	89	339	12.8	58
5	M3	917	104	586	7.4	51
6	M4	970	110	620	7.0	84

[a]ZLI-2293/dopant=10/3 was used as host liquid crystal. [b]Central reflected wavelength (nm) before and after UV irradiation. [c]Reflected bandwidth (nm) before and after UV irradiation. [d]Pitch (nm) before and after UV irradiation. [e]Helical twisting power before and after UV irradiation (μm^{-1}). [f]$T_{Ch\text{-}I}$=transition temperature from cholesteric to isotropic phase. [g]Phase separation. [h] 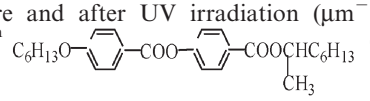 (S-811).

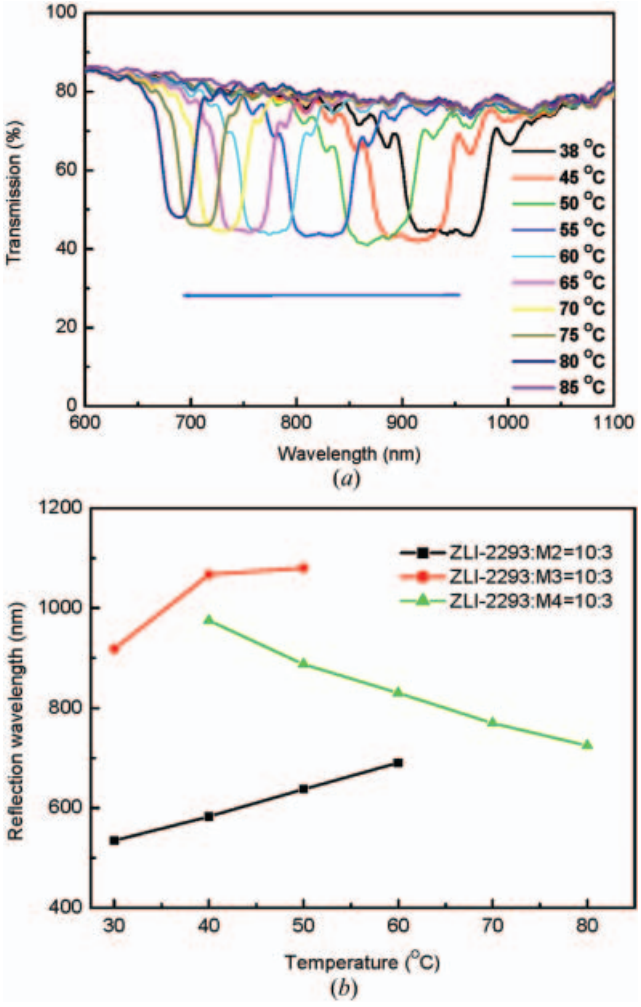

Figure 2. (a) Effect of temperature on cholesteric LC cell (ZLI-2293/M4=10/3); (b) thermal stability of the cholesteric LC cells with various chiral dopants.

centre in the menthyl group the configuration was maintained. All chiral compounds in table 1 containing a menthyl group revealed left-handed specific rotation.

In order to investigate the photochemical tuning effect of the chiral monomers end-capped with menthyl groups on the cholesteric LC cells, chiral monomers M1 to M4 were added to commercially available nematic LC ZLI-2293 to induce cholesteric LC phases. As depicted in figure 1, cholesteric LC cells with various reflecttion bands were fabricated. Furthermore, as seen in entry 2 of table 2, the addition of M1 resulted in a phase separation, whereas entry 3 shows that the addition of M1 with commercially available S811 improved the compatibility between the dopants and LCs. The results suggest that molecular length and polarity may affect the intermolecular forces between the dopants and the LCs leading to phase separation and varying helical twisting power (HTP) inductions. It can be seen in entries 1–6 in table 2 that UV irradiation caused no significant variation in the reflected bands.

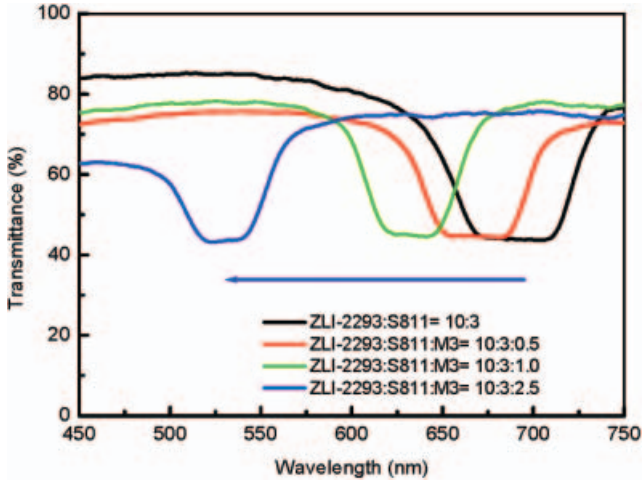

Figure 3. Effect of the M3 doping on the reflection band of cholesteric LC cells.

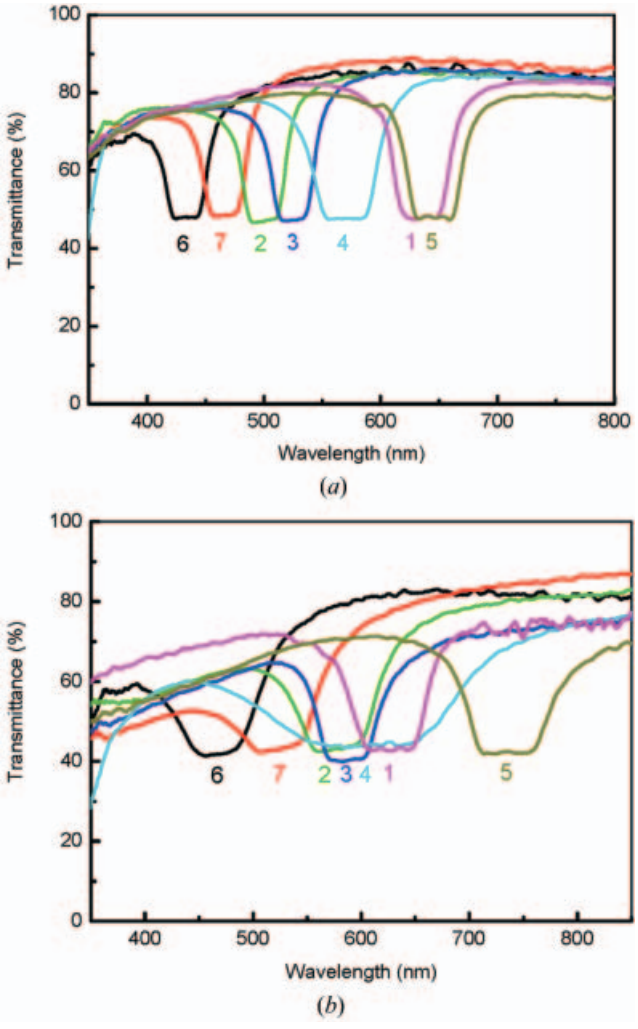

Figure 4. Reflection bands of cholesteric cells (a) before and (b) after UV polymerization; numbers denote cells in table 3.

The results suggest that without the existence of a photoinitiator, UV irradiation did not induce significant polymerization. The addition of dopants into the LC may disturb the molecular interaction leading to a decrease in the clearing temperature ($T_{Ch\text{-}I}$). In contrast, in entry 6, the addition of M4 seemed to increase the clearing temperature of the cell. The longer molecular structure of M4, with a biphenyl and three carboxylic internal groups, might have increased the molecular interaction and the compatibility between M4 and the LC molecules.

Figure 2 shows the thermal stability of the cholesteric LC cells with chiral monomers. Figure 2 a shows that for the LC cells with M4, an increase in the cell temperature induced blue shifts of the reflection bands, which were shifted from the infrared to a visible light region. The thermal effects were compared with dopants of M2 and M3 and are summarized in figure 2 b. For M2 and M3, depending on the dopants added, an increase in the cell temperature caused red shifts. The results suggest that helical twisting structure was induced by the chiral dopants; heat treatment might alter the polarity of the chiral dopants and the molecular interaction between the dopants and the LCs, leading to variation of the twisting pitches.

It was found that the addition of chiral dopants into nematic LCs can induce both right-handed and left-handed helical cholesteric textures [27] independent of *R*/*S* and (+)/(−) of chiral dopants. Until now, the induction of right/left helical structures through chiral dopants has been difficult to predict from the *R*/*S* and (+)/(−) of the chiral dopants only. In order to prepare a cholesteric LC cell with a visible reflected band, commercially available chiral S811 with nematic ZLI-2293 was used as a host. Figure 3 depicts the effect of concentration of M3 on the reflection band. It was observed that an increase in M3 concentration shifted the reflection band to the blue side. This suggests that

Table 3. Variation in the properties of cholesteric LC cells before and after UV polymerization.[a]

Entry	Chiral monomer	Before UV				After UV				
		λ_o[b]	$\Delta\lambda$[c]	p[d]	$T_{Ch\text{-}I}$[e]	λ_o[b]	$\Delta\lambda$[c]	p[d]	$T_{Ch\text{-}I}$[e]	$\Delta\lambda$[f]
1	0[g]	633	57	404	67	630	76	400	70	−3
2	M2	500	41	319	53	579	78	370	57	+79
3	M3	525	44	335	60	588	65	376	64	+63
4	M4	565	66	361	64	612	188	391	73	+47
5	M3[h]	643	58	411	66	735	91	470	71	+92
6	M2[i]	433	39	277	54	469	79	300	59	+36
7	M2[j]	464	35	296	51	537	82	343	54	+73

[a]ZLI-2293/S811/M_x/BAHB/BME=10/3.3/0.38/0.4/0.1 mixture was used. [b]Central reflected wavelength (nm) before and after UV irradiation. [c]Reflected bandwidth (nm) before and after UV irradiation. [d]Pitch (nm) before and after UV irradiation. [e]$T_{Ch\text{-}I}$=cholesteric to isotropic transition temperature. [f]Difference in $\Delta\lambda_o$ between before and after UV irradiation, '+' red shift, '−' blue shift. [g]With no other chiral dopant. [h]S811=3.0. [i]M2=0.76. [j]M2=0.57.

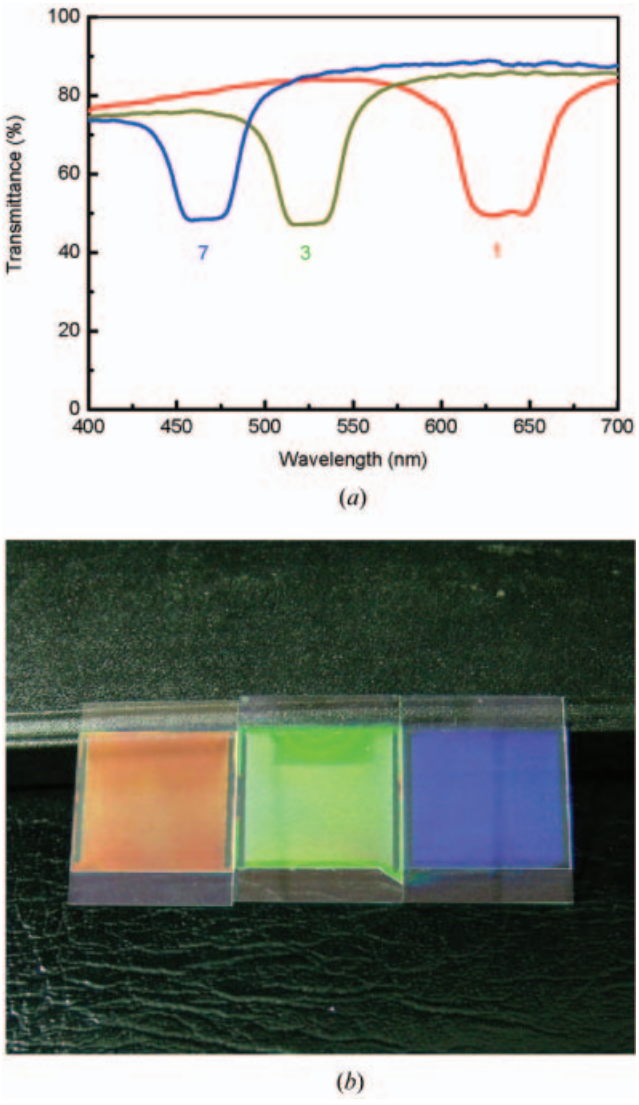

Figure 5. (a) Effect of various chiral dopants on the reflection band of cholesteric LC cells; (b) appearance of RGB reflected colours.

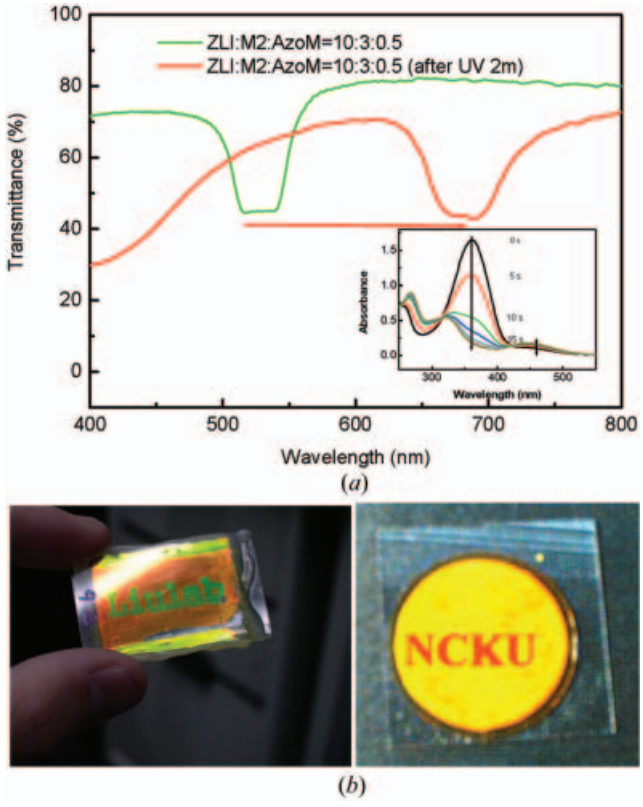

Figure 6. (a) UV-vis spectra of cholesteric LC cell before and after UV irradiation; (b) real image recording through a mask (ZLI-2293/M2/AzoM=10/3/0.5).

the appearance of the cells was colourful and that the colour could be varied simply by adjusting the concentration of M3.

Figure 4 a shows the effect of addition of the chiral monomers to the host LCs. It was found that the addition of chiral monomers caused blue shifts, whereas in cell 5 a slight red shift was seen. The composition of the cells is summarized in table 3. Figure 4 b shows that the reflection bandwidth of the cells was broadened after sufficient UV polymerization. Polymerization of

Table 4. Effect of photoisomerization of AzoM on the reflection band of cholesteric LC cells.

		Before UV				After UV					
Entry	Chiral dopant	λ_o[b]	$\Delta\lambda$[c]	p[d]	HTP[e]	λ_o[b]	$\Delta\lambda$[c]	p[d]	HTP[e]	$\Delta\lambda$[f]	$T_{Ch\text{-}I}$/°C[g]
1	0:3[a]	936	126	598	7.2	1191	246	761	5.7	+255	69
2	3:0.5	523	74	334	11.5	683	111	436	8.8	+160	54
3	3:0.5	822	80	525	7.3	1070	106	684	5.6	+248	48
4	3:0.5	940	95	601	6.4	890	115	569	6.8	−50	82

[a]ZLI-229/M/AzoM=10/0/3 was used; M2, M3, and M4 were added into entry 2, 3, and 4, respectively. [b]Central reflected wavelength (nm) before and after UV irradiation. [c]Reflected bandwidth (nm) before and after UV irradiation. [d]Pitch (nm) before and after UV irradiation. [e]Helical twisting power before and after UV irradiation (μm^{-1}). [f]Difference in $\Delta\lambda_o$ between before and after UV irradiation, '+' red shift, '−' blue shift. [g]$T_{Ch\text{-}I}$=cholesteric to isotropic phase transition temperature.

the chiral monomers fixed the LCs inside the polymer matrices. The UV light was irradiated onto the top side of the cells during photopolymerization. Accordingly, an energy distribution might exist in the film thickness direction, leading to the formation of gradient pitches and the broadening of the reflection bandwidth. These results are consistent with those reported previously [28]. Variation of the chiral dopant altered the reflected central wavelength. The real appearance of the cells is shown in figure 5. The colours of R/G/B can be obtained by adjustment of the concentration of chiral dopants. Table 3 shows the optical properties of the fabricated sample cells. The data showed that the addition of the chiral dopants slightly decreased the clearing temperature, whereas the UV polymerization broadened the reflection bands. For cell 1, with no added monomer, UV irradiation did not significantly affect the optical properties. Entries 2, 6 and 7 in table 3 show that an increase of M2 concentration shifted the λ_0 to the blue side. In contrast, as seen in entry 5, a decrease of S811 concentration shifted the λ_0 to the red side. The results suggest that the reflected colours of the cholesteric LC cells can be controlled for all visible light by varying the dopant compositions.

The data in table 4 show that the addition of the chiral AzoM to a nematic LC induced an infrared reflection band. Photo-irradiation usually induces a configurational *E*/*Z* isomerization of azo derivatives at the N=N segment. Adding chiral monomers and AzoM to the host LC induced cholesteric phases. Entry 1 in table 4 shows that the UV irradiation caused a red shift. The result due to variation of the reflected central wavelength of the cells before and after UV irradiation was estimated as $\Delta\lambda$, where (+) and (−) denote red shift and blue shift, respectively.

Figure 6 a shows the variation of the UV-Vis spectra of AzoM at 365 nm and the red shift of a cholesteric LC cell with the AzoM from 523 to 683 nm. As shown in figure 7, the bent *Z*-form molecules might have disturbed the arrangement of the LC molecules due to alteration of the helical pitches resulting in the red shift of the reflection band. Figure 6 b shows a real sample cell irradiated with UV light through a figured mask. The irradiated area exhibited a red-shifted colour. The colour at the area with no UV irradiation showed no change in the original reflection band. Figure 7 shows a schematic representation of the effect of photoisomerization of the azo derivatives on the arrangement of LC molecules. Photo-irradiation may alter the rod-like *E*-configuration to the bent *Z*-configuration of AzoM and change the order of the LCs. Depending on molecular interaction between the dopants and LCs, the pitch of

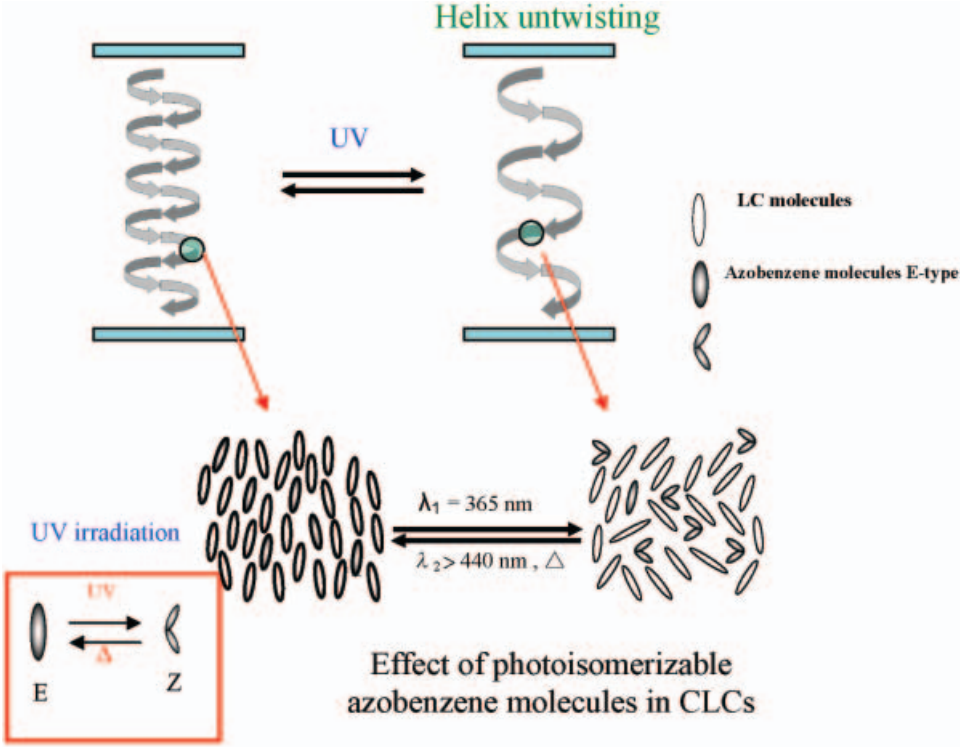

Figure 7. Schematic representation of photo-induced isomerization of AzoM on cholesteric LC cells before and after UV irradiation.

the cholesteric LCs may be shortened or lengthened, leading to a blue shift or red shift of the reflection band. As shown in figure 6, in this case, UV irradiation caused a red shift. The results suggest that with M2 as chiral dopant, the bent *Z*-form of AzoM lengthened the pitch of the cell. The inset spectra in figure 6 a show the variation of UV absorption with UV irradiation time due to photoisomerization of AzoM. The variation observed in the UV region had almost no effect on the variations of the reflection band of cells in the visible region.

To investigate the morphology of the polymer matrix after UV polymerization, the cell glasses were opened along the crossed direction with a diamond cutter. The LCs were washed thoroughly using methanol. Figure 8 shows the SEM photograph of the top view of both top and bottom glass substrates, and the side view of the morphological network structures of the fabricated cholesteric LC cell 1 (entry 1 in table 4). Figure 8 shows that after polymerization, the LCs in the pores of the polymer matrix were removed during the washing with methanol. From the density difference of the residual polymers attached to the glass substrates shown in figures 8 a and 8 b, it could be considered that UV polymerization started from the top side of cells leading to the formation of gradient pitches and different residual polymer densities on the glass substrates. It can be seen in figure 8 c that the LCs were separated and stabilized inside the polymer matrix. The cell was washed thoroughly with methanol to wash out the LCs. In this case, perhaps due to methanol treatment, some low molecular mass gel-like polymers were deformed and washed out. This could be the reason for gradient formation not being seen in figure 8 c. The polymer matrix is expected to support and fix the cell gap between the substrates, especially for the flexible LC films. During the investigation of UV polymerization inside the LC cells, it was found that UV irradiation from the top side of the cell induced a gradient density polymer matrix leading to the formation of a broad band LC cell covering all visible white light. This technique is expected to be used to form a brightness enhancement film which can be applied in the back light module of a LC display. Investigations on the morphology and brightness enhancement of gradient LC films are in progress.

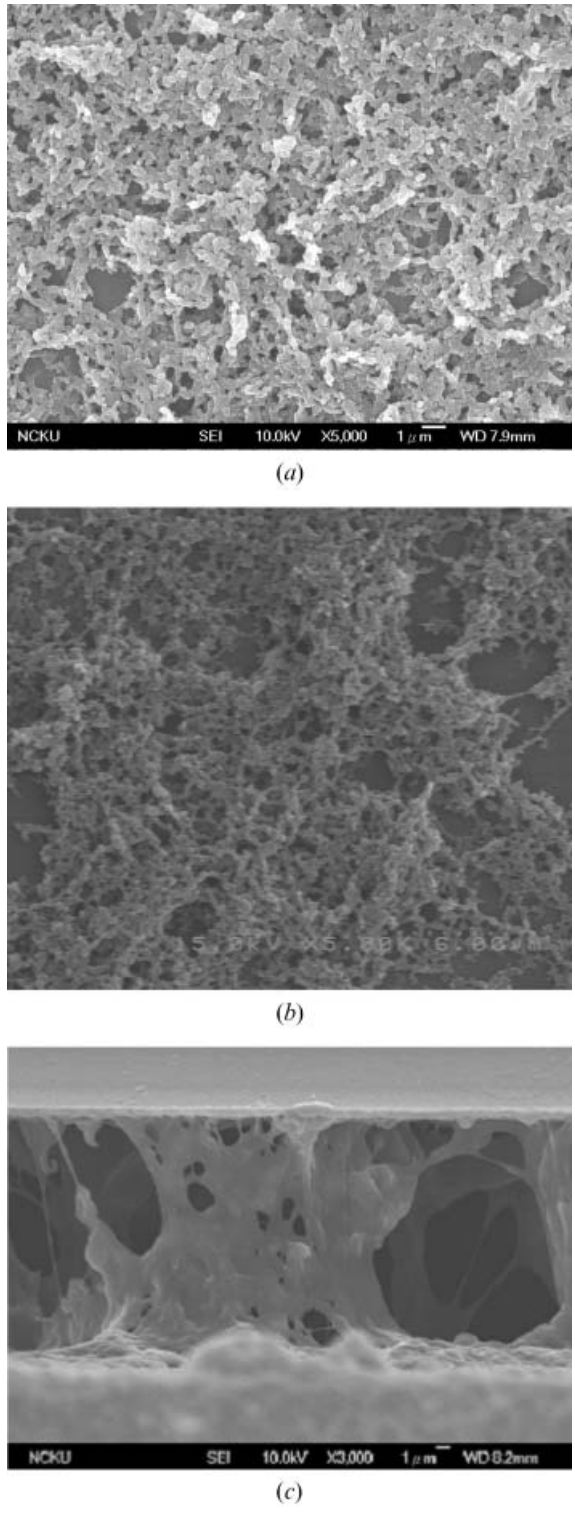

Figure 8. (a) Top view of polymer matrix on the top glass substrate; (b) top view of polymer matrix on the bottom glass substrate; (c) side view of the morphological network structure of the polymer matrix inside a cholesteric LC cell (entry 1 in table 4).

4. Conclusions

The addition of synthesized chiral monomers end-capped with menthyl groups to nematic liquid crystals induced cholesteric liquid crystal phases. The temperature of the cells was found to affect the pitch of the cholesteric LCs leading to a blue or red shift. UV

irradiation changed the *E*-form of AzoM to *Z*-form and altered the pitch of the cells. UV irradiation was found to broaden the reflection bandwidth of the LC cells. Recording text through a mask with UV irradiation on a cholesteric LC cell with synthesized chiral monomers and AzoM was achieved. The results in this investigation showed that RGB reflected colours can be obtained through the use of synthesized chiral compounds containing a menthyl group. The addition of AzoM enables recording of colourful patterns onto cholesteric films using UV exposure.

Acknowledgements

The authors would like to thank the National Science Council (NSC) of the Republic of China (Taiwan) for financial support of this research under Contract No. NSC 94-2216-E006-038.

References

[1] A.Y. Bobrovsky, N.I. Boiko, V.P. Shibaev, K. Schaumburg. *Macromol. Chem. Phys.*, **202**, 2895 (2001).
[2] C. Ruslim, K. Ichimura. *J. Mater. Chem.*, **12**, 3377 (2002).
[3] H.K. Lee, K. Doi, H. Harada, O. Tsutsumi, A. Kanazawa, T. Shiono, T. Ikeda. *J. Phys. Chem. B*, **104**, 7023 (2000).
[4] S. Kurihara, S. Nomiyama, T. Nonaka. *Chem. Mater.*, **12**, 9 (2000).
[5] N. Tamaoki, A.V. Parfenov, A. Masaki, H. Matsuda. *Adv. Mater.*, **9**, 1102 (1997).
[6] M. Brehmer, J. Lub, P. van de Witte. *Adv. Mater.*, **10**, 1438 (1998).
[7] A.Y. Bobrovsky, N.I. Boiko, V.P. Shibaev. *Polym. Sci. A*, **40**, 232 (1998).
[8] P. van de Witte, M. Brehmer, J. Lub. *J. Mater. Chem.*, **9**, 2087 (1999).
[9] E. Sackmann. *J. Am. chem. Soc.*, **93**, 7088 (1971).
[10] T. Yoshioka, T. Ogata, A.M. Zahangir, T. Nonaka, S. Kurihara. *Liq. Cryst.*, **31**, 15 (2004).
[11] T. Yoshioka, A.M. Zahangir, T. Ogata, T. Nonaka, S. Kurihara. *Liq. Cryst.*, **31**, 1285 (2004).
[12] C. Ruslim, K. Ichimura. *J. phys. Chem. B*, **104**, 6529 (2000).
[13] T. Pfeuffer, K. Kürschner, P. Strohriegl. *Macromol. Chem. Phys.*, **200**, 2480 (1999).
[14] N. Hoshino, Y. Matsuoka, K. Okamoto, A. Yamagishi. *J. Am. chem. Soc.*, **125**, 1718 (2003).
[15] M.J. Cook, M.R. Wilson. *J. chem. Phys.*, **112**, 1560 (2000).
[16] J.H. Liu, C.D. Hsieh, H.Y. Wang. *J. Polym. Sci. A*, **42**, 1075 (2004).
[17] J.H. Liu, H.Y. Wang. *J. appl. Polym. Sci.*, **9**, 789 (2004).
[18] J.H. Liu, P.C. Yang. *Liq. Cryst.*, **32**, 539 (2005).
[19] J.H. Liu, P.C. Yang. *Liq. Cryst.*, **33**, 237 (2006).
[20] J.H. Liu, P.C. Yang, T.H. Lin, Y.J. Chen, C.H. Wu, Y.G. Fuh. *Appl. Phys. Lett.*, **86**, 161120 (2005).
[21] J.H. Liu, P.C. Yang. *Polymer*, **47**, 4925 (2006).
[22] J.H. Liu, H.J. Hung, D.S. Wu, S.M. Hong, Y.G. Fuh. *J. appl. Polym. Sci.*, **98**, 88 (2005).
[23] A.Y. Bobrovsky, N.I. Boiko, V.P. Shibaev. *Liq. Cryst.*, **24**, 489 (1998).
[24] H. Hattori, T. Uryu. *Liq. Cryst.*, **26**, 1085 (1999).
[25] M. Portugall, H. Ringsdorf, R. Zentel. *Makromol. Chem.*, **183**, 2311 (1982).
[26] M. Kašpar, V. Hamplová, S.A. Pakhomov, A.M. Bubnov, F. Guittard, H. Sverenyák, et al. *Liq. Cryst.*, **24**, 599 (1998).
[27] S. Pieraccini, M.I. Donnoli, A. Ferrarini, G. Gottarelli, G. Licini, C. Rosini, S. Superchi, G.P. Spada. *J. org. Chem.*, **68**, 519 (2003).
[28] D.J. Broer, G.N. Mol, J.A.M.M. van Haaren, J. Lub. *Adv. Mater.*, **11**, 573 (1999).